Comparison of drug release from PLGA microspheres and novel fibre formulations.

Christopher SJ Campbell[1], M Begoña Delgado-Charro[2], Olivier Camus[1] and Semali Perera[1‡]

[1] Department of Chemical Engineering, University of Bath, UK

[2] Department of Pharmacy and Pharmacology, University of Bath, UK

[‡] Corresponding author. E-mail: S.P.Perera@bath.ac.uk

Abstract

Intraperitoneal cisplatin delivery has recently been shown to benefit ovarian cancer patients. Cisplatin-containing poly(lactide-co-glycolide) (PLGA) microspheres have been proposed for cisplatin delivery. The drug loading of cisplatin containing microspheres produced elsewhere is 3-10 %w. Similar microspheres are reported here with a mean diameter of 38.8 μm, and a drug loading of 11.7 %w, but using ethyl acetate as a safer solvent. In addition, novel formulations of cisplatin-containing solid and hollow PLGA 65:35 (lactide:glycolide) fibres were prepared and are reported here for the first time. PLGA hollow fibres were produced by phase inversion with a high

drug loading of 27 %w. Mechanistic mathematical models were applied to the cisplatin release profiles to allow quantitative comparison of microsphere, solid fibre and hollow fibre formulations. The diffusion coefficient of cisplatin eluting from a typical batch of PLGA microspheres was 4.8×10^{-13} cm^2 s^{-1}; this low diffusivity of cisplatin in microspheres was caused by the low porosity of the polymer matrix. The diffusion coefficients of cisplatin eluting from a batch of PLGA solid fibres and hollow fibres were 6.1×10^{-10} and 3.3×10^{-10} cm^2 s^{-1}, respectively. These fibres allowed the controlled release of high doses of cisplatin over four days and may represent an improvement in slow release technology for treatment of ovarian cancer.

Keywords: cisplatin; poly(lactide-co-glycolide); intraperitoneal; ovarian cancer; fibres; mathematical model

Introduction

Intravenous cisplatin or carboplatin is a popular choice for treating ovarian cancer, in combination with drugs such as paclitaxel in some cases [1]. The most active compound, cis-dichlorodiammine platinum (II) which has come to be known as cisplatin, destroys cancer cells by cross-linking their DNA, which ultimately triggers cell death. Despite its adverse side effects, which also include nerve damage and nausea, about half of all cancer patients receiving chemotherapy are taking platinum drugs.

Another problem with conventional cisplatin delivery is its relatively short lifetime in the bloodstream.

A meta-analysis of eight studies investigating intraperitoneal cisplatin or carboplatin as an addition to standard treatment following surgery has shown an improvement in survival for ovarian cancer patients [1]. PLGA microspheres have been proposed as suitable depot devices for sustained cisplatin delivery [2-9]. Microspheres are formed as the organic solvent is extracted from an emulsion of the polymer solution into the aqueous phase. During solvent extraction some of the drug is able to escape. As a consequence, these microsphere have cisplatin loadings of 3-10 %w. A disadvantage of microsphere formulations is that small microspheres less than 10 μm are readily phagocytosed by immune cells [10, 11]. Phagocytosis of the formulation may increase immunotoxicity or reduce the efficacy of tumour killing.

Instead of entrapping drugs in microspheres, drugs can be incorporated into larger scale fibres. Fibres with controlled porous layers, allow drug release to occur before the biodegradable carrier is reduced to fragments which can be phagocytosed. Meshes of electrospun fibres [12] have been investigated for drug release. The drug release from these structures has not yet been extensively described. In a previous work, hollow fibres filled with drug loaded nanoparticles have been used to control the drug release

[13]. They have reported the dexamethasone and methotrexate drug release profiles from co-polymers such as poly(lactic acid) and ε-caprolactone.

PLGA was selected for this study because it is biocompatible and biodegradable, exhibits a wide range of erosion characteristics, has tuneable porosity and surface area properties and most importantly, is a FDA approved polymer [14]. Polyester PLGA is a copolymer of poly lactic acid (PLA) and poly glycolic acid (PGA). The presence of methyl side groups in PLA makes it more hydrophobic than PGA and hence lactide-rich PLGA co-polymers (e.g. 65:35) are less hydrophilic, more suitable for encapsulating hydrophilic drugs such as cisplatin, and absorb less water preventing rapid loss of drugs. Furthermore, research has demonstrated that PLGA can easily be formulated into the drug carrying devices and can encapsulate a wide range of drugs, peptides or proteins [14, 15].

Here a new form of PLGA device is proposed to overcome these problems and improve drug loading: drug loaded spun solid and hollow fibres of PLGA. For the first time we report the incorporation of the drug directly into spun solid and hollow fibres for continuous manufacture of cisplatin-containing fibres. Rather than finely dispersing the polymer solution in water, it is spun, entering the water bath as a continuous stream. The liquid polymer stream hardens to a solid (phase inversion) as the organic solvent

diffuses into the water. It is proposed that by controlling the conditions of manufacture of these formulations, tailored release profiles could be achieved. In addition, fibres offer the benefits of continuous manufacture which may improve reproducibility and cost to manufacture compared to the batch manufacture of microspheres. Preliminary studies showed that the encapsulation of the hydrophilic drug cisplatin is possible in PLGA (lactide:glycolide) fibres; 50:50, 65:35 and 75:25. The PLGA 65:35 hollow fibre produced by phase inversion gave the highest drug loading compared to other PLGA counterparts and the most suitable controlled drug release profile (*in vitro* study) for cancer care, hence this paper presents the drug depot development using 65:35 PLGA system.

Mechanistic models for studying diffusion of small molecules in matrices based on Fick's laws of diffusion have been available for some time [16]. With the advent of powerful, freely obtainable, open-source software [17], mathematical models can be rapidly and effectively applied to drug release profiles to high accuracy using a standard desktop computer. Statistical methods can be used to objectively identify optimum formulations.

The objectives of this work were (a) to demonstrate the principle that cisplatin fibres could be a promising alternative to microspheres and (b) to perform rigorous

comparisons between the release profiles provided by the formulations. To this aim, mechanistic models were used to estimate the diffusion coefficients of cisplatin in microspheres, solid and hollow fibres.

Materials and methods

Manufacture of microspheres

PLGA 65:35 (Alkermes, Birmingham, USA) molecular weight of 90-140 kDa was dissolved in ethyl acetate to 15 % by weight of dope. Cisplatin powder (50 % by weight of PLGA) (Lianyungang Unionrun Foreign Trade Co., Jiangsu, China) was dispersed into this mixture on a rolling bed. Microspheres were manufactured by oil in water emulsion using a mechanical homogenizer. Polyvinyl alcohol (1 %w) was used to as a suspending agent to lower the interfacial tension between the oil and water. The suspension was stirred at room temperature for four hours to allow solvent evaporation and microsphere hardening. Microspheres were collected by centrifugation at 1200 *g*, washed with distilled water and filtered. Microspheres were then dried overnight over a column of air.

Manufacture of solid fibres

Spun fibres were manufactured by extruding polymer/cisplatin dope through a needle of the spinneret into a water bath and controlling the phase inversion process. The dope consisted of poly(lactide-co-glycolide) (PLGA) dissolved in N-methylpyrrolidone

(NMP), also containing powdered cisplatin in suspension. PLGA 65:35 was dissolved in n-methyl-2-pyrrolidone (NMP) to 18 % by weight of dope. Cisplatin powder (50 % by weight of PLGA) was dispersed into this mixture on a rolling bed in a 20 mL syringe. Cisplatin was added at the same time as PLGA (F1a, F1b) or after the PLGA had completely dissolved (F2). The dope was then extruded through a spinneret needle at 1.0 mL min^{-1} into a water bath. The polymer dope entered the water bath as a continuous stream; solvent diffused out of the nascent fibre into the water bath. A coagulated PLGA fibre containing encapsulated drug is formed due to the rapid partitioning of water-soluble organic solvent from the polymer stream [18]. The fibre was collected using a rotating spindle (14 rpm) to draw the fibre into a second water bath. Fibres were soaked in distilled water for 1 h before being wrapped around a cardboard support and vacuum dried overnight.

Manufacture of hollow fibres

Hollow fibres (H1) were manufactured in the same way as solid fibres but were extruded through a double bore spinneret rather than through the needle. A spinneret is a spinning orifice with two concentric needles [19]. Polymer dope was extruded through the outer orifice at 3.3 mL min^{-1} and distilled water flow through the central orifice at 1.2 mL min^{-1}creating a central bore with a porous skin layer. Air gap of 5cm and bore flow rate of 1.2 ml/min was found to be suitable for encapsulation of cisplatin and controlling the porosity of the structure.

Scanning electron microscopy

Cisplatin solid (F1b, F2) and hollow (H1b) fibres were incubated in distilled water. After 0, 1, 5 and 21 h the water was aspirated, the samples of fibres were oven dried overnight at 30°C. Samples were cut into small sections (0.3 cm), then pressed onto carbon tabs on specimen plates. Samples were carbon coated prior to imaging. Scanning electron microscopy (SEM) images were recorded using a JEOL JSM 6310 electron microscope at 5 keV accelerating voltage.

Mercury Intrusion Porosimetry

Pore structures of PLGA microspheres and fibres were investigated by mercury intrusion porosimetry (MIP) on a Pascal 140 mercury porosimeter with mercury being forced into the pores of the test samples at elevated pressures.

Backscattered electron imaging

To find the cisplatin distribution, backscattering maps were performed on a JEOL JSM 6310 electron microscope at 15-20 keV accelerating voltage. While SEM detects secondary electrons which are emitted from the carbon coating of the sample, backscattering detects electrons which are reflected directly back from the electron beam by the sample if it meets an electron opaque material such as platinum atoms. Release of cisplatin from solid and hollow fibres was also examined by digital image analysis of SEM and backscattered images. Samples of fibres (each set n=4) were

soaked in distilled water at 30°C for 1, 5.6 or 21 hours and oven dried at 30°C overnight. Unsoaked fibre samples were also placed in the oven to control the effect of temperature. SEM and backscattered images were taken of cross-sections of fibre samples (n = 4). In order to calculate the areas, images were analysed using ImageJ.

X-ray microanalysis mapping

X-ray microanalysis mapping was performed using a JEOL JSM 6310 electron microscope at 5 keV accelerating voltage. X-rays are emitted at characteristic frequencies by atoms which are excited by the electron stream. Maps were generated by collecting the signal corresponding to X-ray frequencies emitted by platinum and chlorine in cisplatin. Co-localised platinum and chlorine suggests that cisplatin is present. No additional preparation was required for X-ray analysis following SEM. X-rays emitted by the excited samples were directly captured in situ using the JEOL JXA8600 Superprobe electron probe microanalyser attachment.

Atomic absorption spectroscopy

Active unbound cisplatin release from delivery devices was quantified using atomic absorption spectroscopy (AAS) at 265.9 nm, the frequency corresponding to platinum absorption [20]. The instrument, a Perkin Elmer Model 3110, was manually calibrated using a working curve. The dilution series consisted of twelve platinum standards in

HCl 2.0 M from 1.000 mg mL^{-1} to 0.001 mg mL^{-1}. The method was validated by dissolving powdered cisplatin in water for comparison with the standard.

Release profiles for microspheres (8 mg mL^{-1}), solid fibres (5 mg mL^{-1}), and hollow fibres (5 mg mL^{-1}) were determined in 1 mL of distilled water at 37°C for each measurement. At each time point the vials containing microspheres were centrifuged 500 g for 3 min to pellet the microspheres, allowing the release medium to be aspirated. A 0.7 mL aliquot of release medium was analysed using AAS; the remaining liquid was discarded. Pre-warmed distilled water (1 mL) was used to replace the release medium for the next measurement. Samples were dried using heated ceramic crucibles and digested with *aqua regia* (3 vol concentrated HCl: 1 vol concentrated HNO_3) at 105°C until near dryness twice. Once dry the samples were dissolved in 1.0 mL HCl, 2 M. Each microsphere release experiment was performed in triplicate; the fibres release experiments were performed with six replicates. Blank microspheres and fibres were manufactured and received equivalent treatment and release conditions as the drug-loaded formulations. No cisplatin was detected in release medium from any of these controls.

Mathematical models

The cisplatin release data were analysed using empirical and mechanistic models. Cisplatin release profiles from different batches were here compared using non-linear

mixed effects modelling [21]. This approach treats the inter-batch and intra-batch variation separately.

First order models are also appropriate for use as semi-empirical models for studying drug release from depots [22, 23]. It can be assumed that the driving force for mass transfer is proportional to the difference between the outer surface concentration and the concentration of analyte in an analyte-rich region [24]. Equation 1 describes drug release from a depot under sink conditions where the concentration of drug in solution, $M1(t)/v_1$, is determined by the amount of drug in the depot, $M2(\infty)$, and the release constant, k_{21}.

$$\frac{M1(t)}{v_1} = M2(\infty)\cdot\left(1 - e^{-k_{21}t}\right) \quad (1)$$

For some depot formulations the initial burst of drug release can occur faster than predicted by a single first order process. In these conditions equation 1 is not appropriate. A skewed drug distribution could arise if drug crystals are preferentially encapsulated at or near the surface of the depot. Release would be faster than expected if it had been assumed that the drug was homogeneously distributed in the matrix. A second exponential term can be added to equation 1 to represent the depot as a slow

releasing component of the drug. On the other hand, the three compartment model may be more suitable to show the release of two pools of drugs in the fibre into the solution.

However, adding parameters to any model will generally reduce the residual error of the fit. Increasing the number of parameters in a model decreases the degrees of freedom. The more complex model should not be used unless the improvement in predicting power justifies the reduction in degrees of freedom. One effective method for determining whether this is true is to calculate Akaike's Information Criterion (AIC) [25]. AIC allows comparison of mathematical models of data by trading off the number of parameters used against the residual error. AIC values can only be used to compare different models of a dataset, not between datasets. The model with the lowest AIC is likely to have the optimum balance between simplicity and good predictive power. AIC can be used in conjunction with hypothesis testing methods such as analysis of variance/covariance during model comparison. The advantage of AIC is that unlike hypothesis testing there is no concern that the sequence of analysis will affect the results.

Equation 2 describes drug release from a depot under sink conditions consisting of two independently releasing pools. The concentration of drug in solution, $M1(t)/v_1$, is determined by the amount of drug in the two pools, $M3(\infty)$ and $M4(\infty)$ and the release

constant of the two pools, k_{31} and k_{41} respectively. AIC was used to determine whether using the second pool was justified for each dataset.

$$\frac{M1(t)}{v_1} = M3(\infty)\cdot\left(1-e^{-k_{31}t}\right) - M4(\infty)\cdot\left(1-e^{-k_{41}t}\right) \quad (2)$$

Good mechanistic diffusion models have been derived from Fick's law. These models assume sink conditions to simplify the calculations. Mechanistic models can be used to calculate the diffusivity of the drug in the matrix. The diffusivity reflects the properties of the matrix ignoring the shape and porosity of the matrix. Differences observed must be due to the microscopic differences in the matrix structure.

Equation 3 is the Higuchi model [26] where $M(t)$ is the amount of drug released across the exposed area, A, after time t, D is the diffusivity of the drug in the matrix medium, $M(\infty)/V$ is the total amount of drug ($M(\infty)$) initially present in the matrix per unit volume (V) and C_s is the solubility of the drug in the solvent.

$$\frac{M(t)}{A} = \sqrt{DC_s\left(2M(\infty)/V - C_s\right)\cdot t} \quad (3)$$

The Higuchi model can be simplified to obtain a linear model as a function of the square root of time with a single parameter related to the diffusivity. As the model is only defined for one dimension, the drawback of this method is that the approximation is only valid for early release and becomes skewed by complete release profiles.

Fick's Second Law states that the rate of change of concentration in a matrix is proportional to the rate of change of concentration gradient at that point. Using boundary conditions and rewriting Fick's Second Law to define the morphology of the depot, a diffusion model can be derived for any regularly shaped device. For spherical devices, such as microspheres the amount of drug released ($M(t)$) is predicted to have the form shown in equation 4 [16] where n are the terms in the Taylor series expansion, D is the diffusivity of the drug in the matrix, t is time since the start of release and R is the radius of the microsphere.

$$M(t) = M(\infty) \cdot \left(1 - \frac{6}{\pi^2} \sum_{n=1}^{\infty} \frac{1}{n^2} \exp\left(-n^2 \pi^2 \frac{D}{R^2} t\right)\right) \quad (4)$$

The cylindrical model (equation 5) incorporates the geometry of the solid fibre [16]. The diffusivity (D) of solid fibres can be calculated assuming that the fibres are infinitely long, perfect cylinders with radius, a, equal to the mean radius of the fibre.

The Taylor series is calculated using α_n as the series of positive roots of the Bessel function of the first kind of zero order divided by a ($J_0(a\alpha_n) = 0$).

$$M(t) = M(\infty)\cdot\left(1 - \sum_{n=1}^{\infty}\frac{4}{(a\alpha_n)^2}\exp\left(-D\alpha_n^2 t\right)\right) \quad (5)$$

For a hollow fibre there are different boundary conditions that must be considered. It is assumed that the fibres are infinitely long, perfect hollow cylinders with inner radius, a, and outer radius, b. This model (equation 6) incorporates the effect of the release of drug from the inner surface of the hollow fibre. The Taylor series is calculated using α_n as the series of positive roots from the convolution of the Bessel functions of the first and second kind of zero order divided by a and b respectively ($J_0(a\alpha_n)Y_0(b\alpha_n) - J_0(b\alpha_n)Y_0(a\alpha_n) = 0$).

$$M(t) = M(\infty)\cdot\left(1 - \frac{4}{(b^2 - a^2)}\sum_{n=1}^{\infty}\frac{J_0(a\alpha_n) - J_0(b\alpha_n)}{\alpha_n^2\left\{J_0(a\alpha_n) + J_0(b\alpha_n)\right\}}\exp\left(-D\alpha_n^2 t\right)\right) \quad (6)$$

More complicated models have been developed incorporating terms for particle size distribution or tortuosity of voids in the matrix [27] but the effect of adding additional terms to the model is not justified unless large improvements of explanatory power can

be made. Models incorporating the effect of polymer degradation have not been included in this study as the rate of degradation is slow compared to the rate of drug release for this system.

Datasets were fitted to exponential (equation 1), biexponential (equation 2), Fick's First Law [26] (equation 3) and Fick's Second Law [16] (equation 4, 5 or 6) models using R software [17]. Relative fits to the different models were compared using AIC.

Results and discussion

Depot morphology

Microspheres, solid fibres and hollow fibres were manufactured as described in the methods section and observed using SEM and mercury porosimetry to identify morphological features. X-ray microanalysis was used to check that the cisplatin was well dispersed in the matrix.

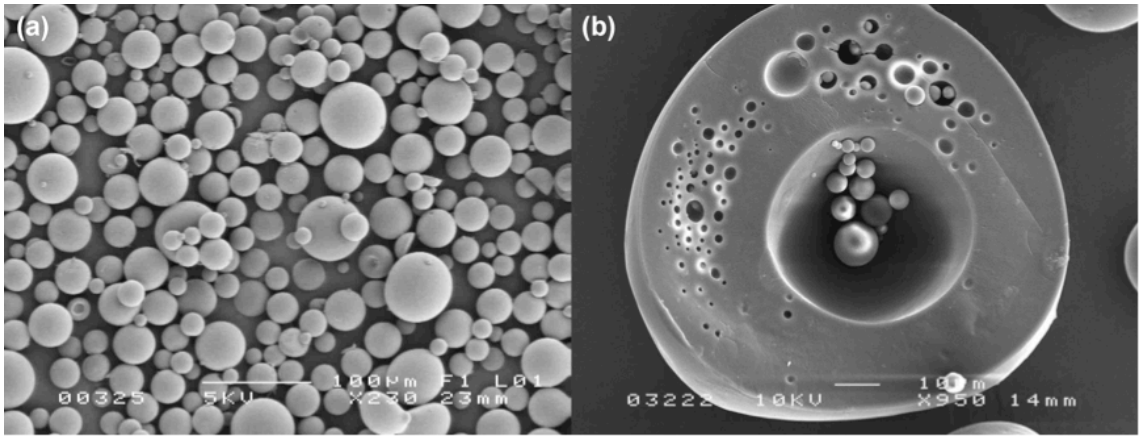

Figure 1. SEM image showing PLGA 65:35 microspheres.

Microspheres which had fractured during freeze drying were observed in some images. Scale bar is 100 and 10 μm.

PLGA 65:35 microspheres were 10 to 100 μm in diameter (Figure 1a). The median particle diameter was 38.8±1.4 μm when measured by laser scattering (data not shown). Figure 1b shows a microsphere which had fractured during freeze drying, revealing the internal structure. Fractured microspheres were composed of solid matrices with small internal pores. Although some pores were connected the majority were discrete. Some microspheres appeared to have engulfed other microspheres with shell-like pores surrounding some regions of a microsphere. This type of structure reflects the properties of the emulsion from which the microspheres were formed. Droplets of oil phase dispersed in the aqueous continuous phase could be expected to contain droplets of water themselves. The low porosity of these microspheres suggests that diffusion of

drug will be slow as there are few aqueous channels to allow paths of lower resistance to drug escape.

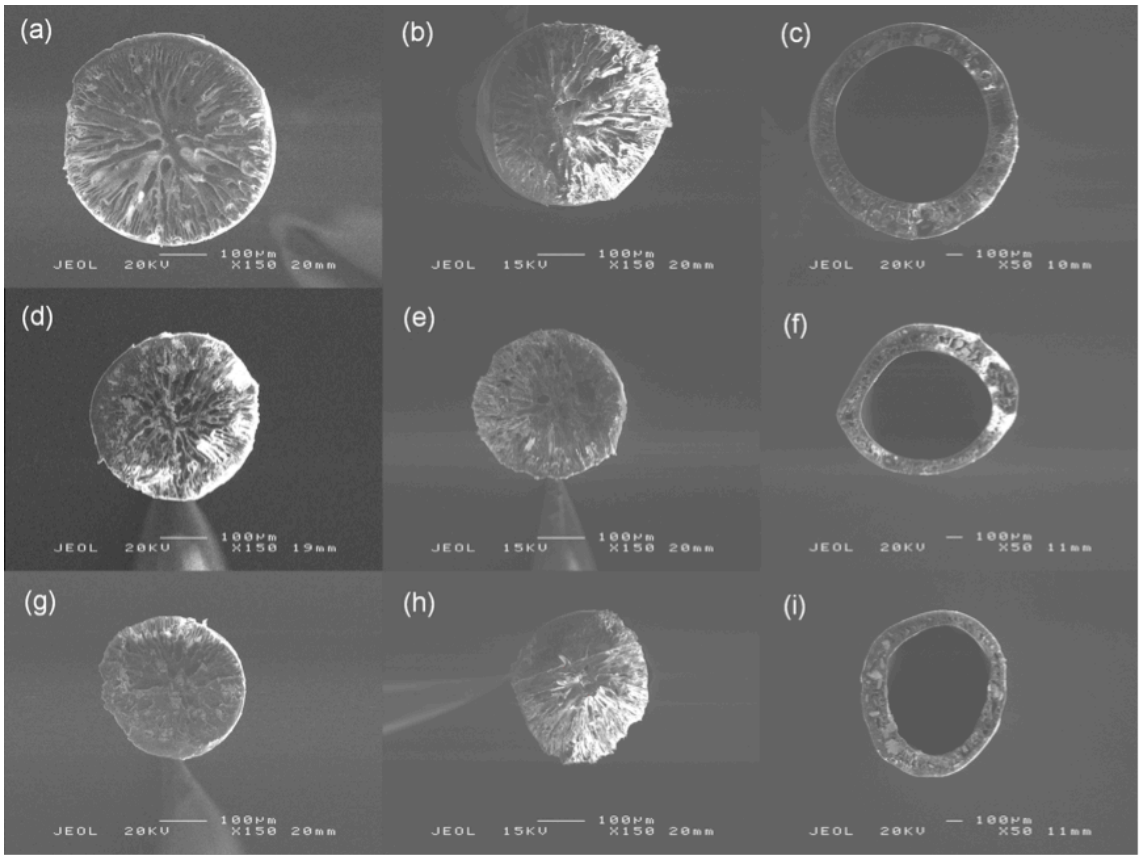

Figure 2. SEM images of PLGA 65:35 fibres and effect of drug release in distilled water.

SEM images of F2 (a, d, g), F1b (b, e, h) and H1b (c, f, i) fibres before soaking (a, b, c), and after soaking for 5 h (d, e, f) and 21 h (g, h, i). Scale bar is 100 µm. (F2) = Solid fibre with cisplatin added to clear PLGA solution; F1b = solid fibre with Cisplatin, PLGA and NMP all mixed at once; H1b is hollow fibre.

Figure 2 shows a cross-section through PLGA 65:35 solid (F1b, F2) and hollow fibres (H1b). The matrices of solid and hollow fibres are similar to each other but different from microspheres (Figure 1). This suggests that matrix solidification is different during emulsion and phase inversion processes. Since immiscible organic solvents such as ethyl acetate partition into the water phase slowly, the matrix of microspheres is well formed and solid. Conversely, water-soluble organic solvents such as NMP rapidly partition out of the stream of dope. As the polymer loses its solvent and water begins to enter the fibre, voids are left in the structure, creating finger-like macro voids with a porous skin layer.

An alternative theory of the pore formation is that they are formed during the drying process. As more solvent is extracted during phase inversion, the oil phase becomes a poorer solvent to the polymer chains. The chains become less extended in solution and interact more with each other [28] causing the glass transition temperature to increase. Since the glass transition temperature is higher and the polymer chains are moving less, the diffusivity of the solvent in the oil phase decreases. This decreases the rate at which the solvent is extracted. The outer layer of the droplet solidifies first, leaving a molten centre. Depending on how long the droplet is exposed to water the droplets of polymer may completely then harden as the remaining solvent dissolves away or retain a viscous

liquid centre. When the formulation is vacuum dried the remaining solvent is extracted, reducing the volume of the core and causing voids to form.

The pores in the fibre structure act as a faster alternative pathway for cisplatin release compared to the more dense structure of microspheres. This may be an advantage for fibres since their larger physical size may otherwise hinder drug release too much.

Results of the Mercury Intrusion Porosimetry (MIP) analysis revealed that the hollow fibre (porosity of 84.3 ± 0.05%; total pore surface area of 60.28 ± 0.1 $m^2 g^{-1}$) was 33.30 ± 0.5% more porous and has larger total pore surface area than the microspheres (porosity of 56.29 ± 0.05 %; total pore surface area of 11 ± 0.1 $m^2 g^{-1}$). The analysis indicated that the solid fibre has a porosity of 74.0 ± 0.05% and total pore surface area of 65.28 ± 0.1 $m^2 g^{-1}$. While the surface areas of the PLGA hollow and solid fibres were as would be expected, the PLGA denser beads showed significantly less surface area than would be anticipated, suggesting mercury pressurisation may have some effect on fragile pore structure of the beads, therefore it is possible that the pore size determined for spheres using MIP may have been skewed. The low porosity of the PLGA spheres may also be due to the formation of the denser structure during the emulsion polymerisation process and possible deformation of accessible pores by the mercury pressurization process. The hollow and solid fibres were shown to have skin average

pore diameters of 30.90 ± 0.05 nm and 25.60 ± 0.05 nm, respectively. From their pore size distributions, it was seen that the structure of both fibres contained macro-pores (pore sizes > 50 nm) and meso-pores (pore sizes between 2 to 50 nm). The denser structure of the PLGA spheres was also confirmed by SEM results.

Solid and hollow fibres were analysed by backscattered electron imaging to generate high-resolution images of the electron dense regions within the matrix of the fibre.

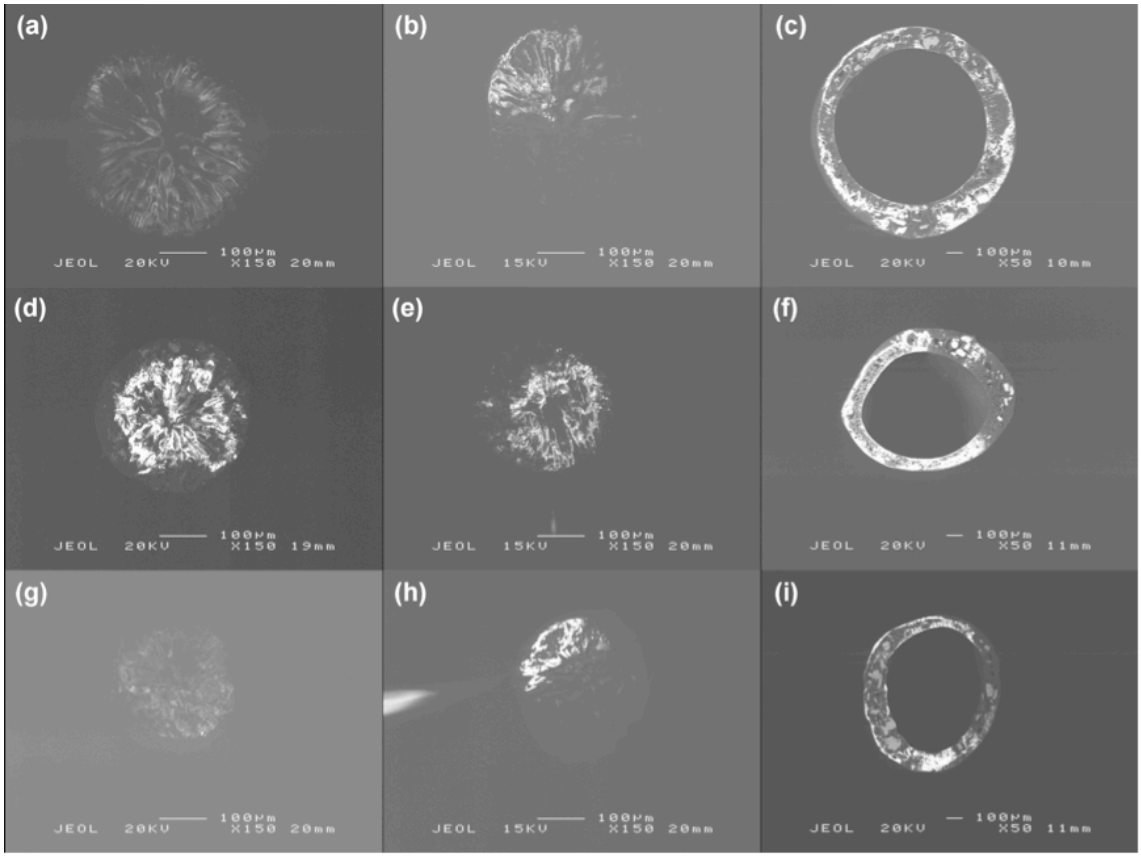

Figure 3. Backscattered electron images of PLGA 65:35 fibres and effect of drug release in distilled water.

Backscattered images of F2 (a, d, g), F1b (b, e, h) and H1b (c, f, i) fibres before soaking (a, b, c), and after soaking for 5 h (d, e, f) and 21 h (g, h, i). Sample images correspond to Figure 2. Scale bar is 100 μm. (F2) = solid fibre formed with Cisplatin added to clear PLGA solution; F1b = solid fibre formed with Cisplatin, PLGA and NMP all mixed at once; H1b is hollow fibre.

Figure 3 shows the backscattered electron images corresponding to the SEM images in Figure 2. The area of cisplatin was estimated by setting the threshold of the backscattered image to just before random speckles appeared in the threshold mask. The

area of the mask helped to estimate the amount of drug present in the fibre qualitatively. Examining the proportion of the area of the fibre occupied by a high cisplatin density, it could be observed that the amount of cisplatin present decreased with time.

In Figure 4 the normalised area was plotted against soaking time. In this case, a mean area was used to calculate the normalised area because each sample was an independent sample instead of the same sample measured repeatedly. The cross-section of the fibres decreases during drug release (Figure 4). In addition, the area of cisplatin decreases. The fibre becomes more hydrophilic as it degrades. This allows water to enter the finger-like pores. The shrinkage seen here may be caused by the walls becoming progressively crushed by the surface tension between water on opposite pore walls. The amount of drug loading in the drug delivery matrix seems to have played a significant role on the rate and duration of drug release. Matrices having higher drug content possess a larger initial burst release than those having lower content because of their smaller polymer to drug ratio.

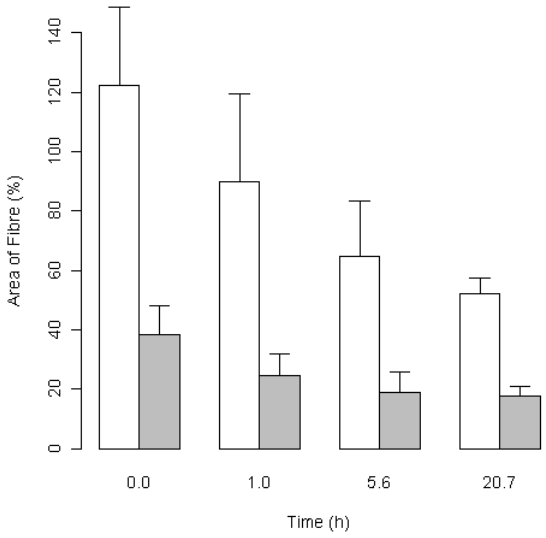

Figure 4. Decrease in the area of PLGA 65:35 hollow fibres (H1b) and the strongly backscattering area.

Normalized area (white) and area corresponding to percentage of fibre cross-section containing cisplatin (grey) (n = 4). Error bars show standard deviation $p = 0.95$.

X-ray microanalysis at regions of high backscattered electron density confirmed that platinum was present. In addition, solid fibres were analysed by X-ray microanalysis mapping to confirm that the signals corresponding to the platinum and chlorine co-localized across a wider area.

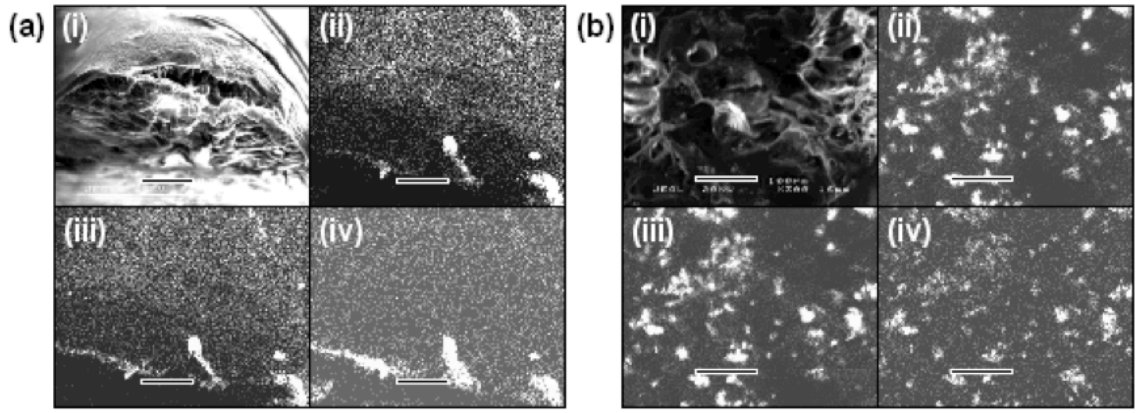

Figure 4. (i) SEM and (ii, iii, iv) associated X-ray maps of (a) F1a and (b) F2 PLGA 65:35 cisplatin solid fibre.

X-ray maps collected at wavelengths corresponding to platinum (ii) Mβ and (iii) Lα bands and (iv) chlorine Kα band. (Scale bar is 100 μm).

Figure 5 shows an SEM (top left) of solid fibre cross-sections and X-ray maps of the same area for F1a and F2 fibres. The wavelengths of the X-rays collected correspond to the strongest wavelengths of platinum (Mα/Mβ at 2.1 keV and Lα at 9.4 keV) and chlorine (Kα at 2.6 keV). Strong platinum and chlorine signals were recorded for F1a and F2 fibres but not cisplatin-free fibres (data not shown).

From the co-localisation of peaks at wavelengths corresponding to platinum Mβ and Lα bands and chlorine Kα bands in images of F1a and F2 fibres it can be inferred that cisplatin is the major electron reflecting species in the fibre. The cross-section of F1a shows a few large cisplatin crystals with many smaller particles dispersed throughout

the fibre. As for F2 fibres the platinum and chlorine bands overlap but appear as large crystals rather than smaller finely dispersed crystals.

Cisplatin was added to the dope early for F1a fibres and late for F2 fibres. In the case of solid fibres (F1a, F1b), the dope solution was made by adding cisplatin crystals to PLGA polymer pellets and then adding NMP solvent to dissolve the polymer while for F2 dope was made by mixing cisplatin to clear PLGA solution. Cisplatin in F1a fibres is more finely dispersed than for F2 fibres where individual crystals can be seen. It is possible that crystals of cisplatin had time to disaggregate in the F1a dope and become well dispersed during the extended mixing period.

Depot release profiles

Rigorous statistical modelling of drug release data can facilitate comparison and optimization of formulations but such analyses are rarely published by experimentalists. The widespread use of desktop computers and the free availability of powerful software [17] makes comprehensive statistical analysis within the reach of all investigators.
The data reported by other groups suggests that cisplatin is stable in aqueous solutions hence active cisplatin release profiles for PLGA 65:35 depots were quantified using the AAS method reported by Ma et al. [20].

The cisplatin release profile of PLGA 65:35 microspheres was determined for known masses of microspheres in distilled water by atomic absorption spectroscopy. The level of batch variation was determined to be low using nonlinear mixed effects modelling [21]. This powerful modelling technique treats each independent batch as having a fixed deviation from the population mean in addition random errors involved when making measurements. Applying the linear driving force (LDF) model (equation 1) using nonlinear mixed effects enables population information about the samples to be determined, generating estimated standard deviations as well as the values of the model parameters: the mass of releasable cisplatin, $M2(\infty) = 11.3 \pm 0.63$ mg and the release constant, $k_{21} = 5.27 \pm 3.23 \times 10^{-6}$ s^{-1} (mean ± standard deviation). These values are similar to those calculated using non-linear least squares fitting (Table 1).

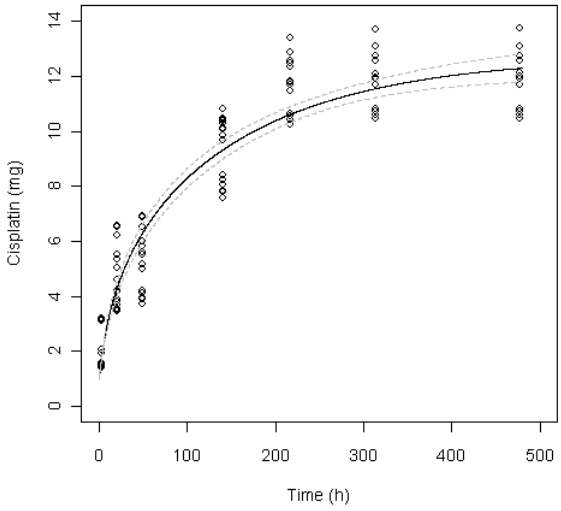

Figure 6. Cisplatin release from PLGA 65:35 microspheres.

Cumulative cisplatin release from equivalent of 100 mg of PLGA 65:35 microspheres (M1a-e) into distilled water over twenty days (n = 5). Lines show Fick's Second Law model (equation 4). Dashed lines show confidence intervals of fit, p = 0.95.

Figure 6 shows cisplatin release from PLGA 65:35 microspheres. These release profiles are typical of cisplatin lactide and glycolide polymer microspheres produce by a range of different routes reported by other groups [18]. These data are shown here fitted to the Fick's Second Law release scheme (equation 4). The mechanistic model derived from Fick's second law for spherical structures had a higher AIC than the empirical models. This suggests that other processes than simple diffusion contribute to diffusion from microspheres. The diffusion coefficient, $D = 4.8\times10^{-12}\pm1.5\times10^{-13}$ cm^2 s^{-1} was determined from D/R^2 in equation 4 using the mean microsphere radius of 19.4 μm. In

addition, the data were fitted to the other models, equations 1-3 (Table 1). From Higuchi kinetics (equation 3) the diffusivity was calculated as $2.0\times10^{-11}\pm8.9\times10^{-15}$ cm^2 s^{-1} (mean ± standard error). Higuchi kinetics overestimates the diffusion coefficient of systems when using total release profiles. It is derived assuming an infinite depot therefore it is only appropriate for describing initial diffusion controlled release. The empirical models (equations 1 and 2) had the best explaining power (lowest AIC). This may mean that wetting, swelling or degradation of the microspheres may play a role in controlling drug release.

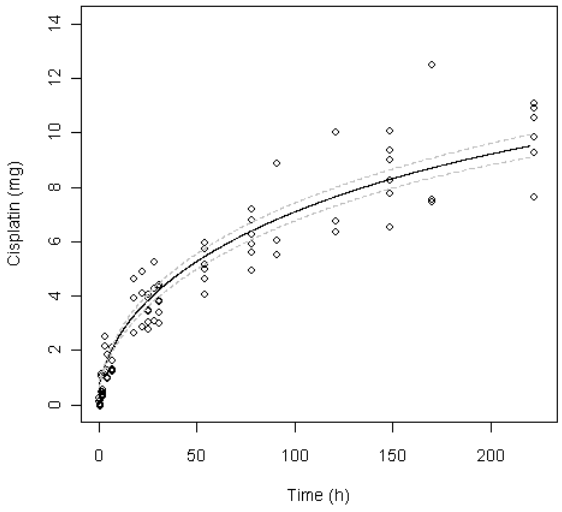

Figure 7. Release of cisplatin from PLGA 65:35 solid fibres.

Cumulative release of cisplatin from equivalent of 100 mg of PLGA 65:35 solid fibres (F1a) into distilled water over ten days (n = 3, 6). Solid line shows Fick's Second Law model (equation 5). Dashed lines show confidence intervals of fit, p = 0.95.

Figure 7 shows cisplatin release from PLGA 65:35 F1a solid fibres. These data are shown here fitted to the Fick's Second Law release scheme (equation 5). This model was as likely to describe the data (similar AIC, Table 1) as the empirical models (equations 1 and 2). This suggests that drug release from solid fibres is controlled by diffusion. Fibres manufactured from a dope to which cisplatin was added after the polymer had dissolved (F2) had a higher drug loading than the other batches (and microspheres) but showed additional variance in the release profile (not shown). Images of the cross-section of F2 fibres show heterogeneous distribution of large cisplatin crystals in the matrix (Figure 2). The variation observed in the release profile is probably caused by this poor dispersion of drug. For the other batches (F1a, F1b) the cisplatin was added at the same time as the polymer meaning that the drug had more time to become well dispersed.

Analysing F1a fibres using Higuchi kinetics the diffusivity of cisplatin in the fibre matrix was $2.7\times10^{-9}\pm2.2\times10^{-12}$ cm^2 s^{-1} (mean ± standard error). This value is two orders of magnitude greater than the diffusivity calculated using Higuchi kinetics for microspheres. This difference could be caused by open pores in the fibre allowing faster diffusion than would occur in a more dense membrane. The Fick's second law model

(equation 5) described the data well and predicted a diffusion coefficient of $6.1\times10^{-10}\pm1.3\times10^{-10}$ cm^2 s^{-1}.

The release profiles of H1a and H1b fibres were determined as for solid fibres. Figure 8 shows release of cisplatin from two independently manufactured batches of hollow fibres. The release profiles of both batches were similar with high drug loading of over 20 %w with drug release for 200 h. This timescale of release is similar to that of microspheres and solid fibres. H1b fibres had a higher drug loading than H1a fibres. Non-linear mixed effects modelling of the linear driving force model (equation 1) calculated that the mass of releasable drug in 100 mg fibres was $M2(\infty) = 23.9\pm3.1$ mg and were released at a rate defined by the release constant, $k_{21} = 4.9\pm0.12\times10^{-6}$ s^{-1} (mean ± standard deviation). Using non-linear least squares to find Crank's solution for a hollow cylinder, diffusivity was $3.3\times10^{-10}\pm3.3\times10^{-11}$ cm^2 s^{-1} for H1a fibres and $3.0\times10^{-10}\pm2.8\times10^{-11}cm^2$ s^{-1} for H1b fibres.

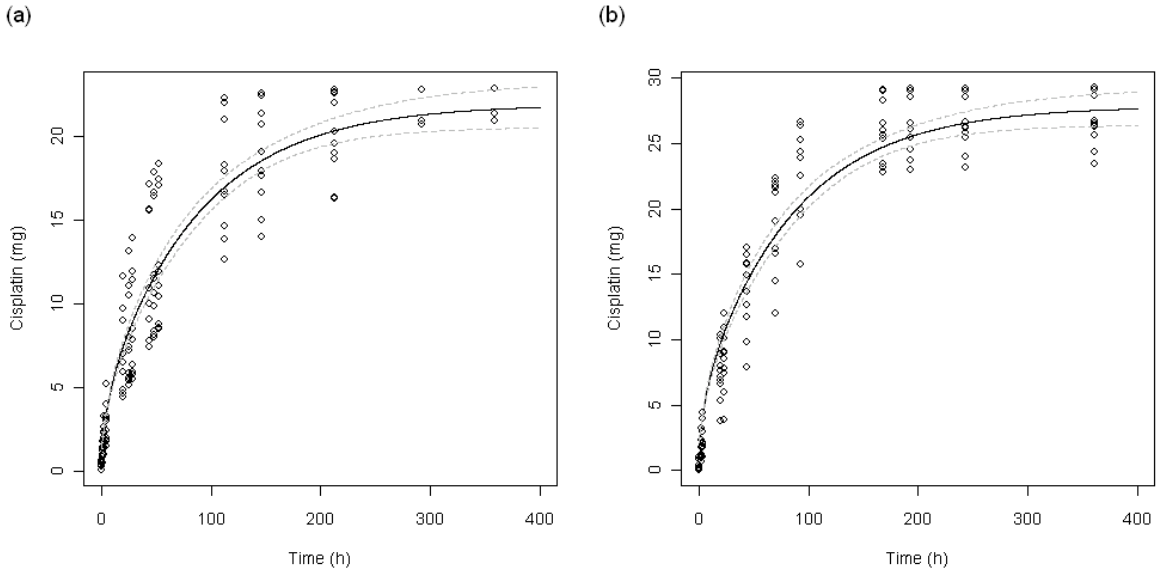

Figure 8. Release of cisplatin from PLGA 65:35 hollow fibres.

Cumulative release of cisplatin from 100 mg of two independent batches of PLGA 65:35 H1a (o) and H1b (□) hollow fibres. Lines show Fick's Second Law model (equation 6). Dashed lines show confidence intervals of fit, p = 0.95.

Table 1. Table of drug release model parameters for PLGA 65:35 microspheres (M1a-e), solid fibres (F1a) and hollow fibres (H1a, H1b)

Parameter values shown ± standard error. * Diffusivity calculated for spherical model from D/R^2 using R = 19.4 μm.

Equation	Parameter	M1	F1a	H1a	H1b
1	LDF $M2(\infty)$ (mg)	11.7±0.24	10.1±0.41	20.8±0.52	27.1±0.44
	LDF k_{21} ($\times 10^{-6}$ s^{-1})	3.95±0.31	4.06±0.40	5.02±0.33	4.78±0.25
	AIC LDF	372	286	673	542
2	2LDF $M3(\infty)$ (mg)	2.46±0.43	1.99±0.46	2.24±1.03	0.506±0.540
	2LDF $M4(\infty)$ (mg)	9.85±0.40	9.88±0.72	19.2±0.95	26.7±0.62
	2LDF k_{31} ($\times 10^{-4}$ s^{-1})	1.05±0.46	0.475±0.225	1.55±1.59	7.76±34.7
	2LDF k_{41} ($\times 10^{-6}$ s^{-1})	2.45±0.31	2.05±0.42	3.94±0.53	4.62±0.30
	AIC 2LDF	331	265	667	545
3	Higuchi k ($\times 10^{-2}$ mg $s^{-0.5}$)	1.10±0.023	1.07±0.031	2.25±0.053	2.95±0.057
	AIC Higuchi	428	328	757	663
4-6	Fick $M(\infty)$ (mg)	12.7±0.41	12.1±0.98	21.8±0.70	27.8±0.74
	Fick D ($\times 10^{-11}$ cm^2 s^{-1}) [0]	0.479±0.015*	61.4±13.3	33.1±3.3	29.9±2.8
	AIC Fick	484	275	668	586

Table 1 shows the calculated parameters for equations 1 to 3 for each of the formulations, as well as the derivation of Fick's second law corresponding to the formulation morphology. Hollow fibres show superior drug loading over microspheres and reproducible release characteristics. The diffusivity of cisplatin in the matrix could

be altered by varying the conditions of manufacture of the fibres by altering the viscosity of the polymer, the air gap between the spinneret and the water bath, the temperature of the polymer and water bath or the rate of fibre draw. These variables will alter the rate of partition of the organic solvent into the water bath. The rate of partitioning has an affect on the porosity of the fibre. It should also be noted that continuous manufacture of hollow fibres is easier to scale up than batch microsphere production, meaning that manufacture of therapeutic fibre formulations would be faster, cheaper and more efficient than for batch production of microspheres.

It is important to note that some of the cisplatin becomes inactivated in vivo by binding of aquated cisplatin to nucleophiles such as glutathione, DNA and proteins and only unbound cisplatin is able to cause tumour killing. In order to understand the release profile changes of these three drug depots in the physiological environment, model proteins have been used to investigate the cisplatin binding targets and the results of the findings will be reported in the future. Characterising the profile of concurrent cisplatin release from a polymer depot and binding to protein will improve understanding of the pharmacokinetics of drug release in the physiological environment.

Conclusion

A drug delivery formulation of cisplatin containing poly(lactide-co-glycolide) hollow fibres was produced with a drug loading more than twice that of comparable

microsphere formulations. The release profiles of batches of drug encapsulated hollow fibre were similar with high drug loading of over 27 %w with drug release for 200 h. The diffusivity of cisplatin in the fibre matrix was found to be far greater than the cisplatin diffusivity in microspheres indicating that high drug release rates could be achieved with novel fibre system. Powdered hydrophilic or hydrophobic drugs can be encapsulated within fibres efficiently with minimum drug loss during the controlled phase inversion process. Some difficulties may arise with liquid drug encapsulation and merit further investigation.

Mechanistic mathematical models were applied to the datasets allowing objective, quantitative comparisons of the formulations. These showed that the rate constant of cisplatin release was similar for all three formulation morphologies. Cisplatin containing hollow fibres have the potential to act as an interesting candidate for sustained release studies for palliative care of ovarian cancer and merit further investigation.

Depot delivery of cisplatin to the peritoneum should offer further improvements in efficacy with reduced toxicity to patients with this disease. The proposed fibre design could be easily adapted to carry other types of drugs or even more than one drug at a time, which means that this device would be suitable for targeting most of the tumours as well as ovarian cancer.

Acknowledgements

The authors would like to thank the University of Bath for providing funding for this work, Ursula Potter and Ann O'Reilly in the Centre for Electron Optical Studies for their expertise in electron imaging, Dr Yunhong Jiang in Department of Architecture and Civil Engineering for supporting the mercury porosimetry measurements, and Nicola Tirelli for informative discussions about fibre formation.

References

[1] Jaaback K, Johnson N, Lawrie T. Intraperitoneal chemotherapy for the initial management of primary epithelial ovarian cancer. *Cochrane Database of Systematic Reviews* 2011;11.

[2] Ike O, Shimizu Y, Wada R, et al. Controlled cisplatin delivery system using poly(d,l-lactic acid). *Biomaterials* 1992;13:230-4.

[3] Araki H, Tani T, Kodama M. Antitumor Effect of Cisplatin Incorporated into Polylactic Acid Microcapsules. *Artif Organs* 1999;23:161-8.

[4] Lee YS, Lowe JP, Gilby E, et al. The initial release of cisplatin from poly(lactide-co-glycolide) microspheres. *Int J Pharm* 2010;383:244-54.

[5] Li Y, Lim S, Ooi CP. Fabrication of Cisplatin-Loaded Poly(lactide-co-glycolide) Composite Microspheres for Osteosarcoma Treatment. *Pharm Res* 2012;29:756-69.

[6] Tamura T, Imai J, Matsumoto A, et al. Organ distribution of cisplatin after intraperitoneal administration of cisplatin-loaded microspheres. *Eur J Pharm Biopharm* 2002;54:1-7.

[7] Fujiyama J, Nakasea Y, Osakib K, et al. Cisplatin incorporated in microspheres: development and fundamental studies for its clinical application. *J Control Release* 2003;89:397-408.

[8] Huo D, Deng S, Li L, et al. Studies on the poly(lactic-co-glycolic) acid microspheres of cisplatin for lung-targeting. *Int J Pharm* 2005;289:63-7.

[9] Matsumoto A, Matsukawa Y, Suzuki T, et al. Drug release characteristics of multi-reservoir type microspheres with poly(dl-lactide-co-glycolide) and poly(dl-lactide). *J Control Release* 2005;106:172-80.

[10] Tabata Y, Ikada Y. Effect of the size and surface charge of polymer microspheres on their phagocytosis by macrophage. *Biomaterials* 1988;9:356-62.

[11] Ayhan H, Tuncel A, Bor N, et al. Phagocytosis of monosize polystyrene-based microspheres having different size and surface properties. *J Biomater Sci Polym Ed* 1995;7:329-42.

[12] Zeng J, Xu X, Chen X, et al. Biodegradable electrospun fibers for drug delivery. *J Control Release* 2003;92:227-31.

[13] Polacco G, Cascone MG, Lazzeri L, et al. Biodegradable hollow fibres containing drug-loaded nanoparticles as controlled release systems. *Polym Int* 2002;51:1464-72.

[14] Siegel SJ, Kahn JB, Metzger K, et al. Effect of drug type on the degradation rate of PLGA matrices. *Eur J of Pharm and Biopharm* 2006;64:287-93.

[15] Frank A, Rath SK, Venkatraman SS. Controlled release from bioerodible polymers: effect of drug type and polymer composition. *J Control Release* 2005;102:333-44.

[16] Crank J. *The Mathematics of Diffusion*. 2nd ed. Bristol: Oxford University Press; 1975.

[17] R Development Core Team. *R: A language and environment for statistical computing*. Vienna: R Foundation for Statistical Computing, 2007.

[18] Campbell CSJ. *Poly(lactide-co-glycolide) Devices for Drug Delivery*. PhD Thesis, Chemical Engineering & Pharmacy/Pharmacology, University of Bath, 2008, p 242.

[19] Perera SP, Tai CC. *Hollow Fibres*. Patent WO/2007/007051, UK, 2006.

[20] Ma JG, Stoter G, Verweij J, et al. Comparison of ethanol plasma protein precipitation with plasma ultrafiltration and trichloroacetic acid protein precipitation for the measurement of unbound platinum concentrations. *Cancer Chemother Pharm* 1996;38:391-4.

[21] Pinheiro JC, Bates DM. *Mixed-Effects Models in S and S-PLUS*. Springer; 2004.

[22] Messaritaki A, Blackb SJ, van der Wallec CF, et al. NMR and confocal microscopy studies of the mechanisms of burst drug release from PLGA microspheres. *J Control Release* 2005;108:271-81.

[23] Machida Y, Onishi H, Kurita A, et al. Pharmacokinetics of prolonged-release CPT-11-loaded microspheres in rats. *J Control Release* 2000;66:159-75.

[24] Glueckauf E, Coates JI. Theory of Chromatography. Part IV. The Influence of Incomplete Equilibrium on the Front Boundary of Chromatograms and on the Effectiveness of Separation. *J Chem Soc* 1947:1315–21.

[25] Akaike H. A new look at the statistical model identification. *IEEE Transactions on Automatic Control* 1974;19:716-23.

[26] Higuchi T. Rate of Release of Medicaments from Ointment Bases Containing Drugs in Suspension. *J Pharm Sci* 1961;50:874-5.

[27] Ritger PL, Peppas NA. A simple equation for description of solute release I. Fickian and non-Fickian release from non-swellable devices in the form of slabs, spheres, cylinders or discs. *J Control Release* 1987;5:23-36.

[28] Artursson P, Brown D, Dix J, et al. Preparation of Sterically Stabilized Nanoparticles by Desolvation from Graft Copolymers. *J Polym Sci A* 1990;28:2651-63.